X-ray Absorption Spectroscopic Analysis of Reductive [2Fe-2S] Cluster Degradation in Hyperthermophilic Archaeal Succinate: Caldariellaquinone Oxidoreductase Subunits

ARTICLE *in* BIOCHEMISTRY · JANUARY 2004

Impact Factor: 3.02 · DOI: 10.1021/bi035078h · Source: PubMed

6 AUTHORS, INCLUDING:

Zhongrui Li
University of Arkansas at Little Rock
82 PUBLICATIONS **2,059** CITATIONS
SEE PROFILE

Robert A Scott
University of Georgia
191 PUBLICATIONS **6,335** CITATIONS
SEE PROFILE

X-ray Absorption Spectroscopic Analysis of Reductive [2Fe-2S] Cluster Degradation in Hyperthermophilic Archaeal Succinate:Caldariellaquinone Oxidoreductase Subunits†

Zhongrui Li,*,‡ Jacob E. Shokes,‡ Asako Kounosu,§ Takeo Imai,|| Toshio Iwasaki,§ and Robert A. Scott‡

Department of Chemistry, University of Georgia, Athens, Georgia 30602-2556, Department of Biochemistry and Molecular Biology, Nippon Medical School, Sendagi, Bunkyo-ku, Tokyo 113-8602, Japan, and Department of Chemistry, Rikkyo (St. Paul's) University, Toshima-ku, Tokyo 171-8501, Japan

Received June 23, 2003; Revised Manuscript Received August 26, 2003

ABSTRACT: The biological [2Fe-2S] clusters play important roles in electron transfer and cellular signaling for a variety of organisms from archaea, bacteria to eukarya. The two recombinant hyperthermophilic archaeal [2Fe-2S] cluster-binding proteins, SdhC and the N-terminal domain fragment of SdhB, of *Sulfolobus tokodaii* respiratory complex II overproduced in *Escherichia coli* are thermostable as isolated, but moderately sensitive to reduction with excess dithionite. We used iron K-edge X-ray absorption spectroscopy to monitor the structural changes of their Fe sites in the irreversible [2Fe-2S] cluster degradation process. Regardless of the differences in the cluster-ligating cysteine motifs and the XAS-detectable $[2Fe\text{-}2S]^{2+}$ cluster environments, a complete reductive breakdown of the [2Fe-2S] clusters resulted in the appearance of a new Fourier transform (FT) peak at ∼3.3 Å with a concomitant loss of the Fe−Fe interaction at *ca*. 2.7 Å for both proteins. On the basis of the unambiguous assignment of the 3.3 Å FT peak, our results suggest that a biological [2Fe-2S] cluster breakdown under reducing conditions generally releases Fe^{2+} from the polypeptide chain into the aqueous solution, and the Fe^{2+} might then be recruited as a secondary ferrous iron source for *de novo* biosynthesis and/or regulation of iron-binding enzymes in the cellular system.

Most biological iron−sulfur clusters play important roles in many physiological electron-transfer processes, in place of direct biocatalysts for enzymatic transformation of the substrate (*1*−*6*). However, there are some instances in bacterial and eukaryal systems in which *in vivo* degradation of iron−sulfur clusters is directly coupled to the switching of signal transduction or transcriptional activation processes as a result of protein conformational changes induced by breakdown of the cluster core (*7*−*9*). For example, bacterial SoxRS, a biological oxygen sensor, contains a highly oxygen labile [2Fe-2S] cluster, which is essential for activating the expression of Fur, a global repressor of ferric iron uptake in bacteria (*9*). Other potential sources of *in vivo* cluster degradation in cells and organella include sudden exposure to high levels of hydroxyl radicals, superoxide anion, or nitric oxide (*e.g.*, on pathogenic infections, oxidative stress, and cell apoptosis) (*10*−*12*). Although physiological consequences triggered by cluster breakdown have drawn much attention to biology, pharmacology, and medicine in recent years, possible structural changes that would occur in the immediate surroundings of the biological cluster during various breakdown processes have not been investigated in detail.

The iron−sulfur clusters in respiratory complex II (succinate:quinone oxidoreductase) play important roles in the intramolecular electron-transfer pathway from the peripheral succinate oxidation site to the membrane-bound quinone reduction site, thereby contributing to the central metabolic and aerobic respiratory system of various aerobic organisms. We have recently identified and characterized a novel "Center C" [2Fe-2S] cluster type in SdhC[1] of succinate:caldariellaquinone oxidoreductase (SdhABCD complex) from hyperthermoacidophilic archaeon *Sulfolobus tokodaii* strain 7 [formerly *Sulfolobus* sp. strain 7, JCM 10545 (*13*)] (*14*−*17*). This cluster is bound to a unique cysteine-rich motif arranged in the two repeated sequences (-YXGC-//-CCG-//-PCSXC-), as seen in archaeal and bacterial heterodisulfide reductases, and does not show any typical "$g \sim 1.91$ or 1.94"

† This work was supported in part by Grants-in-Aid from the Ministry of Education, Science and Culture of Japan (15770088 and Priority Areas 11169237) and JSPS BSAR-507 (to T. Iwasaki), by National Institutes of Health Grant GM 42025 to R.A.S., and by financial support to the Research Center for Measurement in Advanced Science of Rikkyo (St. Paul's) University. The XAS data were collected at SSRL, which is operated by the Department of Energy, Division of Chemical Sciences. The SSRL Biotechnology program is supported by the National Institutes of Health, Biomedical Technology Program, Division of Research Resources.

* To whom correspondence should be addressed: Chemical Engineering and Material Science, University of Oklahoma, Norman, OK 73019. Phone: (405) 325-9178. Fax: (405) 325-5813. E-mail: zrli@ou.edu.

‡ University of Georgia.

§ Nippon Medical School.

|| Rikkyo (St. Paul's) University.

[1] Abbreviations: EXAFS, extended X-ray absorption fine structure; Fe−S, iron−sulfur; Frd, fumarate reductase; FT, Fourier transform; SdhB, subunit B of respiratory complex II; SdhB-N, N-terminal [2Fe-2S] cluster binding domain fragment of SdhB; SdhC, subunit C of respiratory complex II; SSRL, Stanford Synchrotron Radiation Laboratory; XAS, X-ray absorption spectroscopy.

10.1021/bi035078h CCC: $25.00
Published on Web 11/22/2003

EPR signal upon dithionite treatment. The equivalent iron−sulfur cluster has not been found in regular bacterial and mitochondrial complexes II with membrane-bound cytochrome *b* (*15*−*17*). Thus, the archaeal Center C is a novel biological [2Fe-2S] cluster system, presumably with unique immediate cluster surroundings (*17*). The oxidized Center C in archaeal recombinant SdhC protein is significantly more thermostable than those of mesophilic [2Fe-2S] proteins, whereas excess sodium dithionite treatment under reducing conditions causes irreversible breakdown of the [2Fe-2S] cluster core on a time scale of minutes to hours, making it possible to follow the cluster degradation process with various spectroscopic techniques (*17*). As an initial step toward understanding its mechanistic process, we have applied iron K-edge X-ray absorption spectroscopy (XAS) to monitor the structural changes of the iron site upon the irreversible cluster degradation of Center C in recombinant SdhC. X-ray absorption near-edge structure (XANES) and extended X-ray absorption fine structure (EXAFS) spectroscopy provide information that is useful in identifying the oxidation state of the metal ion as well as the neighboring atoms and in determining bond lengths, coordination numbers, and the degree of disorder. The development of X-ray fluorescence excitation XAS enables detection of low concentrations of transition metals present in metalloenzyme systems. This element-specific methodology enables one to look at properties of Fe without major interference from other elements. Our results indicate the appearance of a new Fourier transform (FT) peak at ∼3.3 Å upon the concomitant loss of the Fe−Fe interaction in the degradation process. On the basis of the detailed XAS analysis of the 3.3 Å FT peak, we discuss the fate of iron upon breakdown of a biological [2Fe-2S] cluster system in general.

EXPERIMENTAL PROCEDURES

Recombinant SdhC protein and the N-terminally truncated [2Fe-2S] cluster (Center S-1) binding domain (residues 1−127) of SdhB (called SdhB-N hereafter) of the *S. tokodaii* respiratory complex II subunits (GenBank entry AB055061) were purified as described previously (*17*; manuscript in preparation). The purified proteins were concentrated by pressure filtration with an Amicon YM-10 membrane, and further by placing the samples under a stream of dry argon gas, as previously described (*17*). The resultant samples (∼1 mM), containing 30% (v/v) glycerol, were frozen in 24 mm × 3 mm × 2 mm polycarbonate cuvettes with a Mylar-tape front window for XAS analysis. A stock solution of Ti(III) citrate was prepared under strictly anaerobic conditions in an anaerobic chamber (Coy Laboratory Products, Ann Arbor, MI) as described in the literature (*18*, *19*), and used to reduce the SdhC sample in a XAS cuvette for 4 h. The product was subsequently frozen in liquid nitrogen in the same glovebox. $Fe(II)(NH_4)_2SO_4$ and $Fe(III)(NO_3)_3$ were purchased from Nacalai Tesque.

Iron K-edge X-ray absorption spectra were recorded at beamline 7-3 of SSRL (3.0 GeV and 60−100 mA). A Si(220) double-crystal monochromator was used, and the amount of radiation was detuned 50% at 7820 eV to minimize harmonic contamination. The beam size for all experiments was 10 mm × 1.5 mm, and data were collected at a temperature of 10 K, which was maintained by a continuous flow liquid helium cryostat, in the fluorescence yield mode, using an energy-resolving 30-element germanium solid-state array detector (see Table 1). No photoreduction was observed in comparing the first and last spectra collected for a given sample. Energies were calibrated using an internal Fe foil standard, assigning the first inflection point to 7111.3 eV.

Table 1: X-ray Absorption Spectroscopic Data Collection

	Fe K-edge EXAFS
SR facility	SSRL
beamline	7-3
current in the storage ring (mA)	60−100
monochromator crystal	Si[220]-4
detection method	fluorescence
detector type	solid-state array[a]
scan length (min)	20−22
no. of scans on average	8−18
temperature (K)	10
energy standard	Fe foil, first inflection
energy calibration (eV)	7111.3
E_0 (eV)	7120.0
pre-edge background	
energy range (eV)	6790−7075
Gaussian center (eV)	6403
Gaussian width (eV)	630
spline background	
energy range (eV)	7120−7155 (4)
(polynomial order)	7155−7590 (4)
	7590−7825 (4)

[a] The 30-element Ge solid-state fluorescence detector at SSRL is provided by the NIH Biotechnology Research Resource.

The intensities and energies of the 1s → 3d pre-edge features of the protein data were quantified with the fitting program EDG_FIT (written by G. N. George, SSRL), which utilizes the double-precision version of the public domain MINPAK fitting library (*20*). All spectra were fit over the range of 7100−7165 eV. Pseudo-Voigt line shapes of a fixed 1:1 ratio of the Lorentzian to Gaussian contribution were used to model pre-edge features and successfully reproduce the spectra. Functions modeling the background contributions to the pre-edge features were chosen empirically to give the best fit and included pseudo-Voigt functions that mimicked shoulders on the rising edge. For all complexes, a fit was considered acceptable only if it successfully reproduced the data and the second derivative of the data. The pre-edge peak area after the background subtraction was obtained by integrating over a range of 10 eV.

Extended X-ray absorption fine structure (EXAFS) data analysis was carried out by using the EXAFSPAK suite of programs (available from http://ssrl.slac.stanford.edu/exafspak.html). Calibration and background removal were performed according to established procedures (*21*, *22*). The expression representing the K-edge EXAFS formula for an unoriented sample with Gaussian disorder (not including corrections for many-body effects)

$$\chi(k) = \frac{N_i F(k,R_i)}{kR_i^2} \exp(-2k^2\sigma_i^2) \exp\left[-\frac{2R_i}{\lambda(k,R_i)}\right] \sin[2kR_i + \delta_i(k,R_i)]$$

was used to quantitatively analyze the EXAFS oscillations by a curve fitting procedure. Here N_i is the number of scattering atoms (*e.g.*, nitrogen or sulfur) a mean distance R from the absorber atom (in this case iron), with a mean square

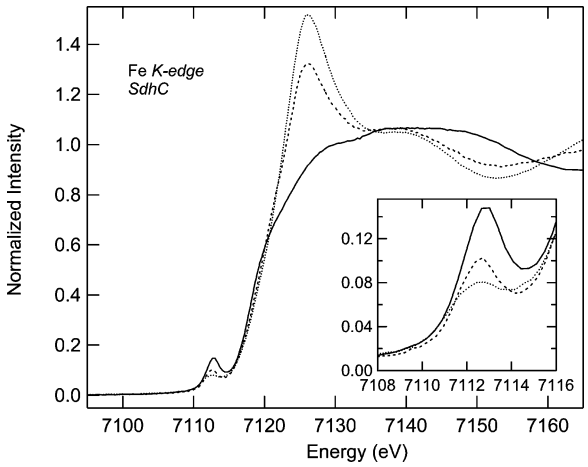

FIGURE 1: Fe K-edge X-ray absorption spectroscopic comparison of SdhC in the oxidized state (—) and after incubation with dithionite for 30 min (- - -) and 4 h (•••). The inset expands the 1s → 3d transition.

deviation in R of σ_i^2 (the Debye−Waller factor), and k is the photoelectron wavenumber. Additional variables that were refined were S_0^2, the passive electron amplitude correction factor for many-body effects, and ΔE_0, the refined correction to the threshold energy, which is assumed to be 7120 eV for the Fe K-edge. The functions $F(k,R_i)$, $\lambda(k,R_i)$, and $\delta(k,R_i)$ are the curved-wave EXAFS amplitude, photoelectron mean-free path, and phase functions, respectively. They were calculated using the *ab initio* code FEFF 7.02 (*23*). A scaled factor S_0^2 of 0.9 was used to fit experimental EXAFS amplitudes with those calculated by FEFF. Correlations between E_0 and R_i, and N_i and σ_i^2, fitting parameters were reduced by weighting the EXAFS data by k^n ($n = 1$, 2, or 3) and simultaneously fitting the differently weighted EXAFS, $k^n\chi(k)$, using a single set of structural parameters. A theoretical $\chi^{calc}(k)$ is constructed whose adjustable structural parameters R_i, N_i, and σ_i^2 are refined against the experimental data by nonlinear least-squares minimization of a reduced F factor. F in particular is somewhat analogous to the crystallographic R factor:

$$F = \frac{\{\sum_i [k^3(\chi_i^{obs} - \chi_i^{calc})]^2/N\}^{1/2}}{(k^3\chi^{obs})_{max} - (k^3\chi_{obs})_{min}}$$

RESULTS AND DISCUSSION

Fe K-Edge XAS Analysis. Archaeal SdhC has the unique cysteine-rich motif and recently has appeared to contain a novel [2Fe-2S]-type Center C that can be reduced by succinate in respiratory complex II (*17*). In the recombinant SdhC protein, Center C was slowly and irreversibly degraded upon dithionite treatment, and its time course was followed by the XAS technique. The Fe K-edge absorption features have been shown to be sensitive to the oxidation state and geometry of the iron atom. The Fe K-edge X-ray absorption spectra reveal a dramatic change in edge shape for SdhC with dithionite treatment (Figure 1). Concomitant with this change is a decrease in the intensity of the 1s → 3d transition at ~7113 eV (inset of Figure 1). The 1s → 3d transition pre-edge features are formally electric dipole forbidden, but gain intensity through an electric quadrupole transition, and

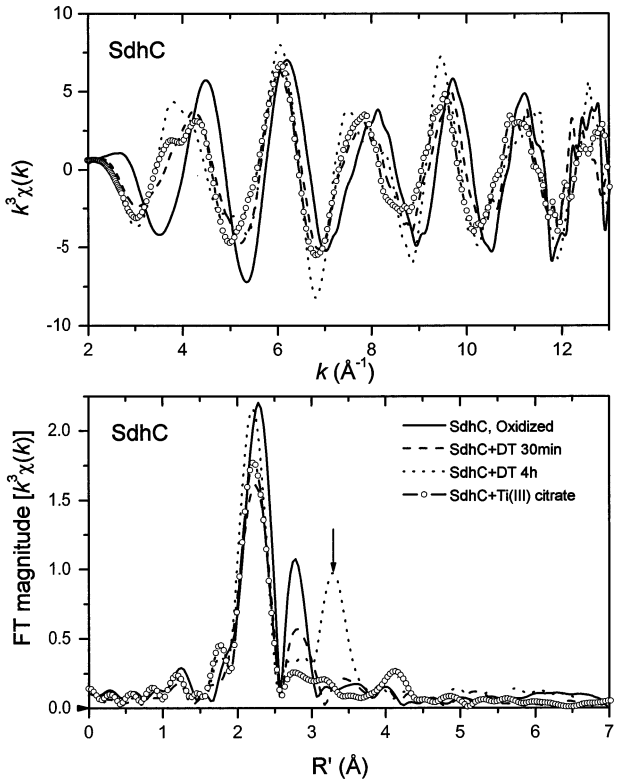

FIGURE 2: k^3-weighted Fe K-edge EXAFS (top) and Fourier transforms (over a k range of 2−13 Å^{-1}, bottom) of oxidized (—), dithionite-treated [30 min (— — —) and 4 h (- - -)], and Ti(III) citrate-reduced (○) SdhC. The ~3.3 Å FT peak is marked with an arrow.

are therefore observed to be weak in centrosymmetric complexes. Since the 1s → 4p electric dipole transition is ~100-fold more efficient than the quadrupole transition, only a few percent 4p mixing is necessary to greatly enhance the intensity of the pre-edge feature. Non-centrosymmetric complexes are therefore observed to have a higher pre-edge intensity.

The total intensity of pre-edge 1s → 3d transition has been shown to increase with decreasing coordination number for iron model complexes because of the loss of inversion symmetry at the iron site (*24*). Analysis of the 1s → 3d pre-edge feature has already been proven to be useful in the determination of the coordination number of iron sites (*24*). Interestingly, the pre-edge peak areas for both oxidized (0.248 eV) and 30 min dithionite-treated (0.203 eV) SdhC samples fall into the regime expected for four-coordinate Fe(III) compounds (*25*). However, the pre-edge peak area of a SdhC sample treated with dithionite for 4 h (0.134 eV) lies in the region for five-coordinate Fe(II) complexes (*26*). Taken together, the change in edge shape and the decrease in intensity of the 1s → 3d transition indicate that the dithionite-treated sample does not contain Fe atoms in a typical [2Fe-2S] electronic environment.

EXAFS Analysis. EXAFS results from the scattering of departing electrons from neighboring atoms. The spectra are exquisitely sensitive to the distance between the scattering atoms and the X-ray-excited atom, out to ~5 Å, and to the nature (atomic number) of the scattering atom. The EXAFS and respective Fourier-transformed (FT) data of both the oxidized and dithionite-treated recombinant SdhC protein are given in Figure 2. In this work, all Fourier transforms were

Table 2: Curve Fitting Results for Fe K-Edge EXAFS[a]

sample, file name (k range), $\Delta k^3\chi$	fit	shell	R_{as} (Å)	σ_{as}^2 (Å^2)	ΔE_0 (eV)	F
		(a) SdhC				
SdhC, oxidized	A1	Fe−S_4	2.24	0.0058	−3.47	0.052
FSDOA (2−13 Å^{-1})		Fe−Fe	2.69	0.0039		
$\Delta k^3\chi = 14.64$	B1	Fe−S_3	2.24	0.0039	−3.26	0.062
		Fe−Fe	2.69	0.0047		
SdhC, dithionite for 30 min	A2	Fe−O_2	2.07	0.0049	−3.79	0.082
FSDRA (2−13 Å^{-1})		Fe−S_2	2.28	0.0049		
$\Delta k^3\chi = 12.33$		Fe−Fe	2.71	0.0069		
	B2	Fe−O	2.05	0.0036	−7.28	0.085
		Fe−S_3	2.27	0.0064		
		Fe−Fe	2.70	0.0068		
SdhC, dithionite for 4 h	A3	Fe−O_4	[2.10]	[0.0046]	[−3.20]	0.054
FSDRB (2−13 Å^{-1})		Fe−S	[2.27]	[0.0014]	[−3.20]	
$\Delta k^3\chi = 16.54$		Fe−S_2	3.26	0.0023	−6.30	
		(b) SdhB				
SdhB, oxidized	A4	Fe−S_4	2.24	0.0059	−2.52	0.076
FSBOA (2−13 Å^{-1})		Fe−Fe	2.71	0.0039		
$\Delta k^3\chi = 14.84$	B4	Fe−S_3	2.24	0.0042	−1.92	0.086
		Fe−Fe	2.72	0.0045		
SdhB, dithionite-treated	A5	Fe−O_4	[2.08]	[0.0067]	[−5.51]	0.075
FSBRA (2−13 Å^{-1})		Fe−S	[2.28]	[0.0012]	[−5.51]	
$\Delta k^3\chi = 13.96$		Fe−S_2	3.23	0.0068	−8.19	
	B5	Fe−O_4	[2.08]	[0.0067]	[−5.51]	0.080
		Fe−S	[2.28]	[0.0012]	[−5.51]	
		Fe−Fe	3.37	0.0044	−24.54	

[a] The errors of data and fits are roughly estimated from the change in the residual factors to be 0.25% for R, 10% for σ_{as}^2, and 4 eV for ΔE_0. No ambiguities in the theoretical standards are included. The shell indicates the type and number of ligands for each shell of the fit. R_{as} is the metal−scatterer distance. σ_{as}^2 is a mean square deviation in R_{as}. ΔE_0 is the shift in E_0 for the theoretical scattering functions. Numbers in parentheses were not varied during optimization. F is a normalized error (χ^2) as defined in the text. The best fits were named with the letter A while others with the letter B.

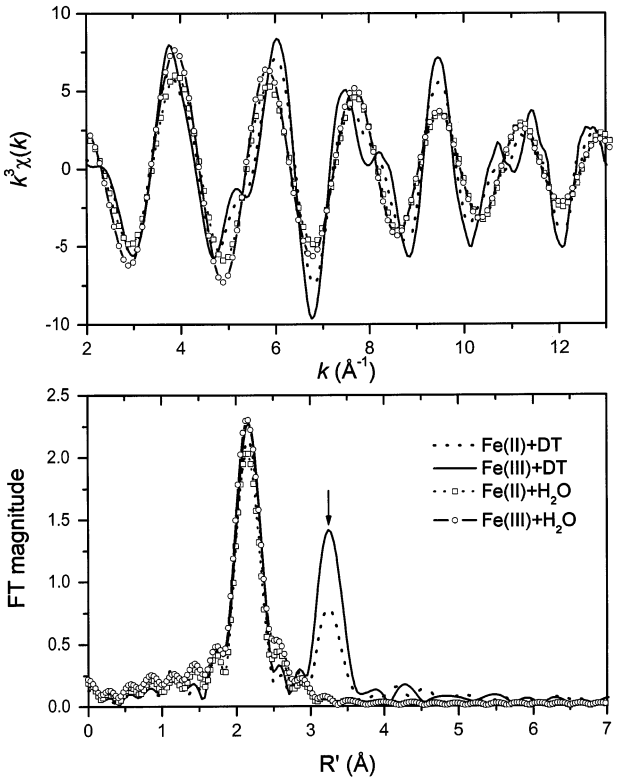

FIGURE 3: k^3-weighted Fe K-edge EXAFS (top) and Fourier transforms (over a k range of 2−13 Å^{-1}, bottom) of Fe(II) and Fe(III) in aqueous solutions with and without dithionite. The 3.3 Å FT peaks were marked with an arrow.

calculated with sulfur-based shift correction. The lower-intensity first-shell FT peaks of dithionite-treated data indicate that there are fewer heavy elements in the first coordination shell than in the oxidized sample. Most interestingly, the dithionite-treated SdhC (4 h) samples are marked by a new FT peak centered at *ca*. 3.3 Å, upon the concomitant loss of that for the Fe−Fe interaction at *ca*. 2.7 Å. These data indicate that the dithionite-treated SdhC does not contain a typical reduced [2Fe-2S] cluster (Figure 2).

Curve fitting analysis of the oxidized sample produces a best fit assuming a coordination environment of four sulfur atoms at 2.24 Å and one iron atom at 2.69 Å (fit A1 in Table 2a). In contrast, the EXAFS data for the 30 min dithionite-treated sample were best fit with two oxygen atoms at 2.07 Å and two sulfur atoms at 2.24 Å and one iron atom at 2.71 Å (fit A2 in Table 2a). The 4 h dithionite-treated sample can be best fit by four oxygen at 2.10 Å and one sulfur atom at 2.27 Å. To analyze the 3.3 Å FT peak, a simulation based on the inner shell was subtracted from the full spectrum. This difference spectrum together with the corresponding FT spectrum was best fit with S (fit A3 in Table 2a). Attempts to include an Fe−Fe scattering shell at ∼3.3 Å were unsuccessful because the refined correction to the threshold energy ΔE is unreasonably large (not shown in Table 2a). This result likely indicates a complete breakdown of the Fe−Fe interaction upon treatment of SdhC with excess dithionite.

Assignment of the New 3.3 Å FT Peak in Dithionite-Treated Archaeal SdhC. We note that the Fe XAS data for SdhC treated with dithionite for 4 h are reminiscent of Fe with mainly (N, O) first-shell ligation (with perhaps a sulfur also, but this could be from a small contamination of undegraded cluster) and more than one S at 3.3 Å. The "second-shell" sulfurs at this distance must be attached to atoms that are directly bonded to the Fe; otherwise, they would be too dynamic to contribute. If a disulfide bound through a sulfur atom to the Fe provides the second-shell sulfur, this would require more than one first-shell sulfur ligand to gain more than one second-shell sulfur scatterer. Thus, a structural unit like the Fe−O−S unit is more likely. A possibility of oxidized cysteines (sulfinic or sulfenic acids) was excluded, since the SdhC protein is reduced by excess dithionite and oxidation of cysteines should not occur under the applied anaerobic conditions. The possibility of SO_2^- bound to Fe(II) through the O is suggested, because it is known that dithionite is in equilibrium in aqueous solution with SO_2^- anion radicals ($S_2O_4^{2-}$ is a dimer of these) and oxidized cysteine thiolates look a lot like dithionite (O_2SSO_2).

To verify this possibility, we first performed XAS experiments with Fe compounds in aqueous solution with excess dithionite to see if a 3.3 Å FT peak appears. Fe(II)$(NH_4)_2$-SO_4 and Fe(III)$(NO_3)_3$ in pure water [purified with a Milli-Q system (Millipore)] were used as model compounds, because they do not contain chloride ion which, when bound to Fe, looks like sulfur bound to Fe and would confuse the XAS analysis. Figure 3 shows the Fe XAS data for the ligand environment of Fe(II) in Fe(II)$(NH_4)_2SO_4$ and Fe(III)$(NO_3)_3$ aqueous solution before and after the addition of excess dithionite. Before the dithionite treatment, the radial distribution functions only display one main FT peak around 2.1 Å due to the oxygen scattering from water. However, upon addition of dithionite, the Fourier transforms of the EXAFS

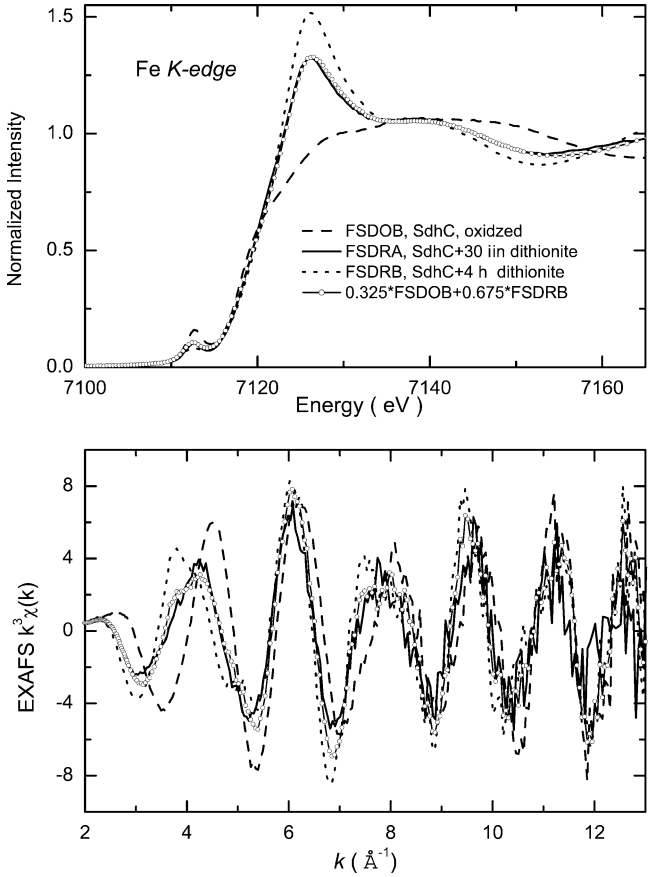

FIGURE 4: XAS simulation of 30 min dithionite-treated SdhC by mixing 32.5% XAS of oxidized (undegraded) SdhC with 67.5% XAS of 4 h dithionite-treated SdhC.

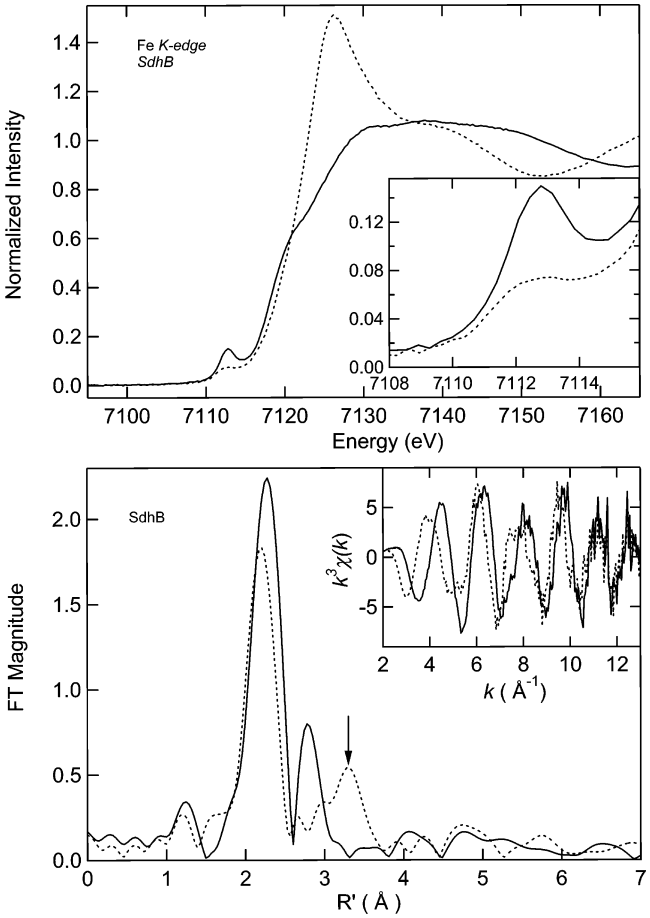

FIGURE 5: Fe K-edge XAS comparison of SdhB in the oxidized state (—) and after incubation with dithionite for 30 min (- - -) (top). The inset expands the 1s → 3d transition. k^3-weighted Fe K-edge EXAFS (insets) and Fourier transforms (over a k range of 2−13 $Å^{-1}$) of oxidized (—) and dithionite-treated [30 min (- - -)] SdhB (bottom). The ∼3.3 Å FT peak is marked with an arrow.

data clearly show a second-shell interaction peak at ∼3.3 Å, as observed for those of the dithionite-treated SdhC protein (Figure 2).

Second, we treated the purified recombinant SdhC protein in a XAS cuvette with excess Ti(III) citrate in an anaerobic chamber (Coy Laboratory Products, Ann Arbor, MI) to ensure anaerobic conditions (*18*, *19*). Ti(III) citrate is a strong reducing reagent containing no sulfur, and has been used for reduction of various iron−sulfur proteins such as nitrogenase Fe protein (*27*). Figure 2 shows no 3.3 Å FT peak for Ti(III) citrate-treated SdhC, despite the reductive breakdown of the [2Fe-2S] cluster as indicated by the loss of the 2.7 Å FT peak for the Fe−Fe interaction.

Together, these results unambiguously show that the reductive degradation of [2Fe-2S]-type Center C in SdhC releases Fe ion into solution, where it is coordinated by the excess dithionite. It also indicates that no polypeptide-bound iron intermediate was formed. In fact, the XAS feature of the 30 min dithionite-reduced SdhC sample can be simulated well by mixing 32.5% XAS of oxidized SdhC with 67.5% XAS of 4 h dithionite-treated SdhC (see Figure 4).

Relevance to Other Biological [2Fe-2S] Cluster Systems. Next, we investigate if another dithionite-sensitive biological [2Fe-2S] cluster also releases Fe(II) into solution upon reductive breakdown of the cluster by XAS. The [2Fe-2S] cluster (Center S-1) in recombinant N-terminally truncated SdhB of the cognate respiratory complex II (namely, SdhB-N) was used as another example of a dithionite-sensitive [2Fe-2S] protein, which was recently overproduced in *Escherichia coli* and has been shown to contain a regular low-potential adrenodoxin-like [2Fe-2S] cluster with complete cysteinyl ligation (*16*; manuscript in preparation). In Figure 5, the 1s → 3d transition pre-edge features at ∼7113 eV of oxidized SdhB-N show that the integrated area (0.246 eV) falls in the range expected for tetrahedral Fe(III) compounds (*25*), while that of 30 min dithionite-treated SdhB-N (0.132 eV) lies in the range for five-coordinate Fe(II) complexes (*26*). Also, the latter's edge feature is very similar of that for SdhC treated with excess dithionite for 4 h.

The curve fitting analysis of the EXAFS data for the oxidized SdhB-N produces a best fit (fit A4 in Table 2b), assuming Fe is coordinated with four sulfur ligands around 2.24 Å and one iron atom at 2.71 Å, consistent with the prediction from the edge analysis. For EXAFS data of the dithionite-treated (30 min) SdhB-N sample, the first FT peak can be best fit with four oxygen ligands at 2.08 Å and one sulfur atom around 2.28 Å in the first coordination shell (fit A5 in Table 2b), which is also consistent with the pre-edge area fitting that predicts a five-coordinate environment of Fe. The presence of the 3.3 Å FT peak and the loss of Fe−Fe interaction at 2.7 Å clearly indicate that a complete reductive degradation of the [2Fe-2S] cluster in SdhB-N releases Fe(II) into aqueous solution, where it is coordinated by the excess dithionite, as observed for the reductive

breakdown of [2Fe-2S]-type Center C in the SdhC protein with different cluster-binding cysteine motifs.

Biological Implication. The [2Fe-2S] cluster in SdhB-N (*14*, *16*) and Center C in SdhC are two succinate reducible high-potential centers detected in the archaeal succinate: caldariellaquinone oxidoreductase complex that differ in their arrangements of the cluster-binding cysteine motifs (*15*−*17*) and the local cluster surroundings. In both cases, however, dithionite treatment causes complete degradation of the [2Fe-2S] clusters, releasing Fe^{2+} into the solvent solution, where it is coordinated by the excess dithionite. This scheme thus seems to be common, at least, for reductive degradation of biological [2Fe-2S] clusters. In Rieske-type [2Fe-2S] clusters, dithionite treatment causes an increase in the average Fe−histidine ligand bond length and the Fe−Fe distance, suggesting small expansion of the cluster core dimensions upon reduction (*28*, *29*). A similar structural expansion of the core dimensions and accompanying structural alterations of the immediate cluster surroundings may trigger the irreversible breakdown of the dithionite-sensitive biological [2Fe-2S] clusters. Our XAS results imply that the ferrous ion released from damaged or aged iron−sulfur proteins and/or enzymes could be chelated, stored, and recruited as a potential secondary iron source on demand of the cellular metabolism and/or perhaps as a potential alert signal for damaged iron−sulfur enzymes, which is also expected for iron released upon oxidative [4Fe-4S] cluster degradation with concomitant formation of a [3Fe-4S] cluster intermediate (*7*, *30*).

REFERENCES

1. Kent, T. A., Dreyer, J. L., Kennedy, M. C., Huynh, B. H., Emptage, M. H., Beinert, H., and Muenck, E. (1982) *Proc. Natl. Acad. Sci. U.S.A. 79*, 1096−1100.
2. Knaff, D. B., and Hirisawa, M. (1991) *Biochim. Biophys. Acta 1056*, 93−125.
3. Ohnishi, T., Moser, C. C., Page, C. C., Dutton, P. L., and Yano, T. (2000) *Struct. Folding Des. 8*, R23−R32.
4. Page, C. C., Moser, C. C., Chen, X., and Dutton, P. L. (1999) *Nature 402*, 47−52.
5. Iverson, T. M., Luna-Chavez, C., Cecchini, G., and Rees, D. C. (1999) *Science 284*, 1961−1966.
6. Lancaster, C. R. D., Kröger, A., Auer, M., and Michel, H. (1999) *Nature 402*, 377−385.
7. Iwasaki, T., Watanabe, E., Ohmori, D., Imai, T., Urushiyama, A., Akiyama, M., Hayashi-Iwasaki, Y., Cosper, N. J., and Scott, R. A. (2000) *J. Biol. Chem. 275*, 25391−25401.
8. Cosper, N. J., Stålhandske, C. M. V., Iwasaki, H., Oshima, T., Scott, R. A., and Iwasaki, T. (1999) *J. Biol. Chem. 274*, 23160−23168.
9. Koh, Y. S., Chung, W. H., Lee, J. H., and Roe, J. H. (1999) *Mol. Gen. Genet. 261*, 374−380.
10. Palatnik, J. F., Valle, E. M., and Carrillo, N. (1997) *Plant Physiol. 115*, 1721−1727.
11. Bianchi, V., Reichard, P., Eliasson, R., Pontis, E., Krook, M., Jornvall, H., and Haggardljungouist, E. (1993) *J. Bacteriol. 175*, 1590−1595.
12. Sellers, V. M., Johnson, M. K., and Dailey, H. A. (1996) *Biochemistry 35*, 2699−2704.
13. Suzuki, T., Iwasaki, T., Uzawa, T., Hara, K., Nemoto, N., Kon, T., Ueki, T., Yamagishi, A., and Oshima, T. (2002) *Extremophiles 6*, 39−44.
14. Iwasaki, T., Matsuura, K., and Oshima, T. (1995) *J. Biol. Chem. 270*, 30881−30892.
15. Iwasaki, T., Wakagi, T., and Oshima, T. (1995) *J. Biol. Chem. 270*, 30902−30908.
16. Iwasaki, T., Aoshima, M., Kounosu, A., and Oshima, T. (1999) in *Flavins and Flavoproteins 1999* (Ghisla, S., Kroneck, P., Macheroux, P., and Sund, H., Eds.) pp 779−781, Agency for Scientific Publishing, Berlin.
17. Iwasaki, T., Kounosu, A., Aoshima, M., Ohmori, D., Imai, T., Urushiyama, A., Cosper, N. J., and Scott, R. A. (2002) *J. Biol. Chem. 277*, 39642−39648.
18. Seefeldt, L. C., and Ensign, S. A. (1994) *Anal. Biochem. 221*, 379−386.
19. Codd, R., Astashkin, A. V., Pacheco, A., Raitsimring, A. M., and Enemark, J. H. (2002) *J. Biol. Inorg. Chem. 7*, 338−350.
20. Garbow, B. S., Hillstrom, K. E., and More, J. J. Argonne National Laboratory.
21. Scott, R. A. (1985) *Methods Enzymol. 117*, 414−459.
22. Cosper, N. J., Stålhandske, C. M. V., Saari, R. E., Hausinger, R. P., and Scott, R. A. (1999) *J. Biol. Inorg. Chem. 4*, 122−129.
23. Zabinsky, S. I., Rehr, J. J., Ankudinov, A., Albers, R. C., and Eller, M. J. (1995) *Phys. Rev. B 52*, 2995−3009.
24. Westre, T. E., Kennepohl, P., DeWitt, J. G., Hedman, B., Hodgson, K., and Solomon, E. (1997) *J. Am. Chem. Soc. 119*, 6297−6314.
25. Roe, A. L., Schneider, D. J., Mayer, R. J., Pyrz, J. W., Widom, J., and Que, L., Jr. (1984) *J. Am. Chem. Soc. 106*, 1676−1681.
26. Randall, C. R., Shu, L., Chiu, Y., Hagen, K. S., Ito, M., Kitajima, N., Lachicotte, R., Zang, Y., and Que, L., Jr. (1995) *Inorg. Chem. 34*, 1036−1039.
27. Angove, H. C., Yoo, S. J., Burgess, B. K., and Muenck, E. (1997) *J. Am. Chem. Soc. 119*, 8730.
28. Tsang, H. T., Batie, C. J., Ballou, D. P., and Penner-Hahn, J. E. (1988) *Biochemistry 37*, 3965−3973.
29. Cosper, N. J., Eby, D. M., Kounosu, A.; Kurosawa, N., Neidle, E. L., Kurtz, D. M., Jr., Iwasaki, T., and Scott, R. A. (2002) *Protein Sci. 11*, 2969−2973.
30. Beinert, H., Holm, R. H., and Muenck, E. (1997) *Science 277*, 653−659.

BI035078H